

## An additional axis for the surface X-ray diffractometer

Masamitsu Takahasi\* and Jun'ichiro Mizuki

JAERI, SPring-8, Kamigori, Ako-gun, Hyogo 678-12, Japan.  
E-mail: mtaka@spring8.or.jp

(Received 4 August 1997; accepted 10 November 1997)

A new surface X-ray diffractometer based on a  $\kappa$ -type diffractometer will be installed in BL14B1, SPring-8. This diffractometer has an additional axis on its detector arm for rotating the receiving slit about the normal of the slit plane, in addition to two axes for positioning the detector. This additional axis is founded on the consideration of the correction factor which has been derived so as to be valid for the  $z$ -axis mode measurement using any incoming and outgoing angles of the X-ray beam. The rotational slit allows accurate measurement of the surface structure factor up to large perpendicular momentum transfer.

**Keywords:** surface X-ray diffraction; diffractometers; correction factors.

### 1. Introduction

With the development of synchrotron radiation sources, surface X-ray diffraction (SXD) has become an important technique for studying surface and interface structures. This technique is based on the measurement of the intensity distribution along the reciprocal lattice rods perpendicular to the surface. Because the reciprocal lattice rods always intersect with the Ewald sphere, the integrated intensity of surface diffraction depends on the rod fraction accepted by the receiving slit in front of the detector.

SXD measurement is often performed in the  $z$ -axis mode where the normal of the sample surface lies in the horizontal plane and coincides with the  $\omega$  axis of the surface X-ray diffractometer. Diffracted beams passing through the receiving slit are integrated with the  $\omega$  rotation of the sample. Two types of diffractometers used for  $z$ -axis mode measurement are shown in Fig. 1. The type (a) is called the six-circle diffractometer (Lohmeier & Vlieg, 1993; Takahasi *et al.*, 1996; Ferrer & Comin, 1995) or the (3+2)\*1 diffractometer (Evans-Lutterodt & Tang, 1995), where '3', '2' and '1' represent the degrees of freedom for the sample, the detector and the whole set-up, respectively. The other type is the so-called  $\kappa$ -diffractometer shown in Fig. 1(b). This is called the (4+2) diffractometer because the sample has four degrees of freedom and the detector has two.

When an  $XY$  slit is used as the receiving slit of these diffractometers, the directions of the  $X$  and  $Y$  blades are usually adjusted to those of the detector motions, namely, the  $\delta$  and  $\gamma$  directions for the (3+2)\*1 diffractometer and the  $\delta$  and  $\eta$  directions for the (4+2) diffractometer. For both diffractometers, the  $X$  and  $Y$  directions are accordant with the in-plane and out-of-plane directions when the outgoing angle of the diffracted beam is zero. In this condition, the rod fraction accepted by the receiving slit is

determined by the blades in the out-of-plane direction. However, as the detector moves around the sample, the  $X$  and  $Y$  blades do not remain aligned to the parallel and perpendicular directions with respect to the sample surface. This causes a complication in that the effective blades of the receiving slit may vary with the geometry of the detector and the sample; the  $X$  blades actually cut off the diffracted beam for one geometry and the  $Y$  blades for another.

The switching of the effective blades can be avoided by rotating the receiving slit about the axis normal to the slit plane. A new (4+2) diffractometer equipped with the 'rotational slit' is currently being constructed and will be installed in BL14B1, SPring-8. In the present paper, the concept of the rotational slit is discussed on the basis of the correction factor which is valid for the  $z$ -axis mode measurement with any incoming and outgoing angles. To focus on the effect of the resolution of the receiving slit, we have assumed in the derivation here that the incident beam is a plane wave and that the sample surface has a perfect two-dimensional periodicity. The effects of the divergence of the incident beam and the broadening of the reciprocal rod due to the finite domain size of the sample surface have been studied by Takahasi (1996).

### 2. Calculation

#### 2.1. General formula

Fig. 2 shows the scattering geometry of the  $z$ -axis mode. The  $\omega$  axis coincides with the  $z$  axis in the figure. The incident beam  $\mathbf{k}_i$  has its in-plane component along the  $y$  axis and an incoming angle of  $\beta_{in}$ . The wavevector of the diffracted beam,  $\mathbf{k}_f$ , is determined by the intersection of the reciprocal rod and the Ewald sphere and makes an angle  $\beta_{out}$  with the sample surface. The angle  $\Phi$  denotes the in-plane projection of the scattering angle  $2\theta$  between  $\mathbf{k}_i$  and  $\mathbf{k}_f$ . The vector  $\mathbf{Q}$  is the momentum transfer defined by  $\mathbf{Q} = \mathbf{k}_f - \mathbf{k}_i$ . The angular deviation of the diffracted beam  $\mathbf{k}_f$  caused by the  $\omega$  rotation is represented by  $(u, v)$ , where  $v$  is such a direction as to increase the outgoing angle  $\beta_{out}$  and  $u$  is the direction perpendicular to both  $v$  and  $\mathbf{k}_f$ .

Using the definitions above, the wave vectors of the incident and diffracted beams are represented by

$$\mathbf{k}_i = (2\pi/\lambda) \begin{pmatrix} \cos \beta_{in} \sin \omega \\ \cos \beta_{in} \cos \omega \\ -\sin \beta_{in} \end{pmatrix}, \quad (1)$$

$$\mathbf{k}_f = \frac{2\pi}{\lambda} \begin{bmatrix} \cos(\beta_{out} + v) \sin(\Phi + \omega) \cos u + \cos(\Phi + \omega) \sin X \\ \cos(\beta_{out} + v) \cos(\Phi + \omega) \cos u - \sin(\Phi + \omega) \sin u \\ \sin(\beta_{out} + v) \cos u \end{bmatrix}, \quad (2)$$

where  $\lambda$  is the wavelength used. If we define  $\mathbf{Q}_0$  as the momentum transfer for  $u = v = \omega = 0$ , the deviation of the momentum transfer  $d\mathbf{Q} = \mathbf{Q} - \mathbf{Q}_0$  is given by

$$d\mathbf{Q} = (2\pi/\lambda) \times \begin{bmatrix} -\sin \beta_{out} \sin \Phi v + \cos \Phi u + (\cos \beta_{out} \cos \Phi - \cos \beta_{in}) \omega \\ -\sin \beta_{out} \cos \Phi v - \sin \Phi u - \cos \beta_{out} \sin \Phi \omega \\ \cos \beta_{out} v \end{bmatrix}, \quad (3)$$

where the linear approximation is employed for the small values  $u$ ,  $v$  and  $\omega$ . The two-dimensional diffraction condition  $d\mathbf{Q}_x =$

$d\mathbf{Q}_y = 0$  yields the following equations,

$$u = (\cos \beta_{in} \cos \Phi - \cos \beta_{out}) \omega, \tag{4}$$

$$v = -(\cos \beta_{in} \sin \Phi / \sin \beta_{out}) \omega. \tag{5}$$

According to the kinematical and the dynamical diffraction theories (Specht & Walker, 1993; Takahashi & Nakatani, 1995), the diffracted intensity for the given incoming and outgoing angles  $\beta_{in}$  and  $\beta_{out}$  is expressed by

$$I_s = I_0 P r_e^2 \lambda^2 (\sin \beta_{in} \sin \beta_{out})^{-1} |F(\mathbf{Q})|^2 / a_0^2, \tag{6}$$

where  $I_0$  is the intensity of the incident beam,  $P$  is the polarization factor,  $r_e$  is the classical electron radius,  $|F(\mathbf{Q})|^2$  is the structure factor for the scattering vector  $\mathbf{Q}$ , and  $a_0$  is the area of the surface unit cell. The integrated intensity evaluated from an  $\omega$ -scan rocking curve is calculated through the integration of (6) weighted with the transmission function of the receiving slit,  $T(u, v)$ . Since  $T(u, v)$  can be expressed as a function of  $\omega$  using (4) and (5), the integrated intensity of an  $\omega$ -scan rocking curve is given by

$$I = [I_0 P r_e^2 \lambda^2 (\sin \beta_{in} \sin \beta_{out})^{-1} |F(\mathbf{Q})|^2 / a_0^2] \int T(\omega) d\omega. \tag{7}$$

Here, it is assumed that the acceptance of the receiving slit is so small that  $|F(\mathbf{Q})|$  can be regarded as a constant value. The transmission coefficient of an  $XY$  slit is expressed by a rectangular function which is unity for  $|X| < \Delta X/2$ ,  $|Y| < \Delta Y/2$  and zero otherwise. For convenience of analytical calculation, however, we employ a two-dimensional Gaussian expressed by (8) instead of the rectangular function,

$$T(u, v) = \frac{4}{\pi} \exp \left\{ - \left[ \frac{4(u \cos v - v \sin v)^2}{\Delta X^2} + \frac{4(u \sin v + v \cos v)^2}{\Delta Y^2} \right] \right\}, \tag{8}$$

which is normalized such that  $\iint T(u, v) dudv = \Delta X \Delta Y$ . Here,  $v$  is the tilt angle of the principal axis of the two-dimensional Gaussian from the  $v$  axis. Replacing  $u$  and  $v$  by  $\omega$  using (4) and (5), we can perform the integration in (7) to obtain

$$I = I_0 P r_e^2 \lambda^2 (\sin \beta_{in})^{-1} |F(\mathbf{Q})|^2 G / a_0^2, \tag{9}$$

where  $G$  is the correction factor represented by

$$G = (2/\pi^{1/2}) \Delta X \Delta Y / [(\sin v a - \cos v b)^2 \Delta X^2 + (\cos v a + \sin v b)^2 \Delta Y^2]^{1/2}. \tag{10}$$

Here,

$$a = \sin \beta_{out} (\cos \beta_{in} \cos \Phi - \cos \beta_{out}), \tag{11}$$

$$b = \cos \beta_{in} \sin \Phi. \tag{12}$$

2.2. (3+2)\*1 diffractometer

As shown in Fig. 1(a), in the  $z$ -axis mode the  $\gamma$  axis of the (3+2)\*1 diffractometer is perpendicular to the normal of the sample surface, irrespective of the  $\delta$  rotation. This means that the tilt angle of the receiving slit,  $v$ , is constantly zero. Hence, the correction factor is expressed by a simple form,

$$G = (2/\pi^{1/2}) \Delta X \Delta Y / (b^2 \Delta X^2 + a^2 \Delta Y^2)^{1/2}. \tag{13}$$

The equation above indicates that the effective blades which determine the length of the rod fraction may vary with the ratio between  $|a \Delta Y|$  and  $|b \Delta X|$ . When the detector system is arranged such as  $|b \Delta X| > |a \Delta Y|$ , the reciprocal rod is cut chiefly by the  $Y$

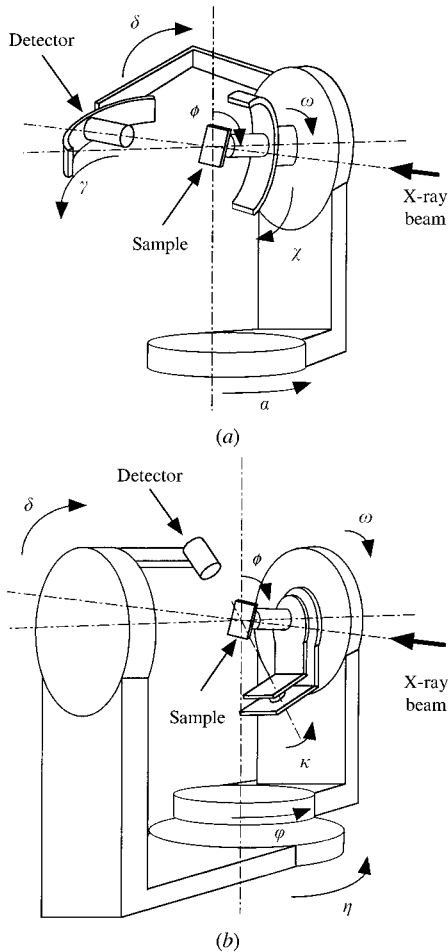


Figure 1 Two types of diffractometer that have been constructed for surface X-ray diffraction experiments. (a) The (3+2)\*1 diffractometer having three axes for the sample ( $\varphi, \chi, \omega$ ), two for the detector ( $\delta, \gamma$ ) and one for the whole setup ( $\omega$ ). (b) The (4+2) diffractometer having four axes for the sample ( $\varphi, \kappa, \omega, \psi$ ) and two for the detector ( $\delta, \gamma$ ).

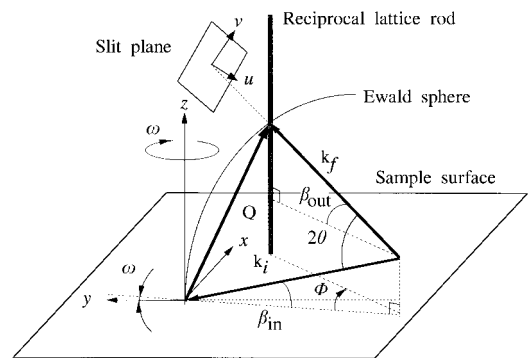


Figure 2 The scattering geometry of the  $z$ -axis mode. The incident X-ray wavevector is  $\mathbf{k}_i$ , the diffracted wavevector is  $\mathbf{k}_f$  and the scattering vector is  $\mathbf{Q}$ . The incoming and outgoing angles are  $\beta_{in}$  and  $\beta_{out}$ , respectively. The scattering angle is  $2\theta$  and its projection onto the sample surface is  $\Phi$ . The angular deviation of the diffracted beam with the  $\omega$  rotation of the sample is denoted by  $X$  and  $Y$ .

blades. In the contrary case that  $|b\Delta X| < |a\Delta Y|$ , the term  $a^2\Delta Y^2$  is dominant in the denominator of (13) so that the  $X$  blades are effective.

### 2.3. (4+2) diffractometer

Unlike the (3+2)\*1 diffractometer, the directions of the  $X$  and  $Y$  blades of the receiving slit on the (4+2) diffractometer do not coincide with the  $u$  and  $v$  axes when  $\beta_{\text{out}} \neq 0$ . This difference is ascribable to the order of the two axes used for the positioning of the detector. The (4+2) diffractometer has the  $\delta$  axis for positioning the detector to the in-plane direction mounted on the out-of-plane axis,  $\eta$ , while the (3+2)\*1 diffractometer has the  $\gamma$  axis on the  $\delta$  axis. The tilt angle of the receiving slit,  $\nu$ , is represented by

$$\sin \nu = \sin \beta_{\text{out}} \sin \Phi / (1 - \cos^2 \beta_{\text{out}} \sin^2 \Phi)^{1/2}. \quad (14)$$

Hence, the correction factor for the (4+2) diffractometer can be obtained by inserting  $\nu$  into (10).

### 2.4. Rotational slit

The tilting of the slit brings a more complicated correction into the measurement using the (4+2) diffractometer than when using the (3+2)\*1 diffractometer. However, if the slit is rotated by  $-\nu$  calculated from (14), the correction factor reduces to the same as that for the (3+2)\*1 diffractometer.

Moreover, we can make the  $Y$  blades always effective, by rotating the receiving slit so that  $a \cos \nu + b \sin \nu = 0$ . As a result,  $\Delta X$  is eliminated from (10) and the following equation is obtained,

$$G = (2/\pi)^{1/2} \Delta Y / (a^2 + b^2)^{1/2}. \quad (15)$$

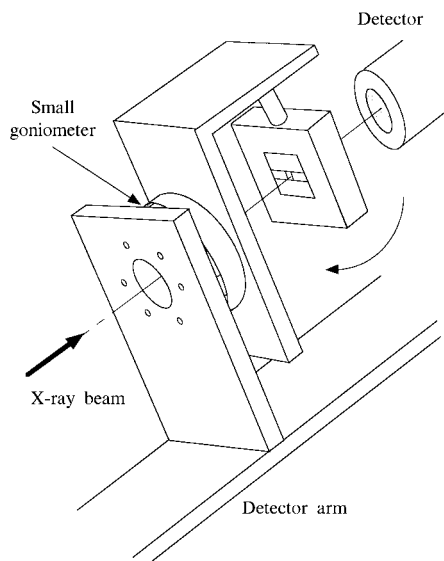


**Figure 3** Illustration of the rotational slit mounted on a surface X-ray diffractometer that is being constructed at SPring-8.

It should be noted that this correction factor is valid for the receiving slit with a rectangular transmission function only by replacing the factor  $2/\pi^{1/2}$  by unity because the  $X$  blades are no longer related to the integrated intensity.

### 3. Discussion

The resolution correction derived in the present work is valid for any incoming and outgoing angles of the X-ray beam, provided that the measurement is performed in the  $z$ -axis mode. It agrees with the existing correction factors which have been conventionally used for surface X-ray diffraction. In the limit of small incoming and outgoing angles, we obtain an identical result to equation (41) of Feidenhans'l (1989), noting that  $\Delta Y = (\lambda/2\pi)\Delta Q_z$ . For large incoming and outgoing angles, our result includes the correction factor derived by Vlieg (1997) for the six-circle X-ray diffractometer with  $\nu = 0$  and  $\Delta Y = \infty$ . The correction factors for the (4+2) diffractometer have been referred to by Evans-Lutterodt & Tang (1995). However, their discussions are restricted to two measurement modes, the  $\beta_{\text{out}} = 0$  mode and the  $\beta_{\text{in}} = \beta_{\text{out}}$  mode, which are special cases of our result. The comparison between the (3+2)\*1 and (2+2) types of diffractometers has been studied by Schamper *et al.* (1993) under the assumption of a small angle of incidence and any outgoing angle. Their result agrees with ours with a small  $\beta_{\text{in}}$  value.

The expression of the correction factor in (10) readily leads to the idea of the rotational slit. Fig. 3 shows a schematic view of the rotational slit which will be mounted on the detector arm of our  $\kappa$ -goniometer. The receiving slit is rotated with a small goniometer having a borehole through which the diffracted beam passes.

This novel axis added to the surface X-ray diffractometer has the advantage of accurate measurement of the intensity distribution along the reciprocal rod. As the outgoing angle  $\beta_{\text{out}}$  increases, the values of  $a$  and  $\nu$  become large according to (11) and (14). Thus, the switching of the effective blades may occur during the rod scan up to large momentum transfer. It is more likely for the (4+2) diffractometer because of the complicated form of the correction factor. The systematic errors resulting from the distortion of the rod profile can be prevented by using the rotational slit.

### References

- Evans-Lutterodt, K. W. & Tang, M. T. (1995). *J. Appl. Cryst.* **28**, 318–326.
- Feidenhans'l, R. (1989). *Surf. Sci. Rep.* **10**, 105–188.
- Ferrer, S. & Comin, F. (1995). *Rev. Sci. Instrum.* **66**, 1674–1676.
- Lohmeier, M. & Vlieg, E. (1993). *J. Appl. Cryst.* **26**, 706–716.
- Schamper, C., Meyerheim, H. L. & Moritz, W. (1993). *J. Appl. Cryst.* **26**, 687–696.
- Specht, E. D. & Walker, F. J. (1993). *J. Appl. Cryst.* **26**, 166–171.
- Takahashi, T. & Nakatani, S. (1995). *Surf. Sci.* **326**, 347–360.
- Takahashi, M. (1996). Thesis, University of Tokyo, Japan. (In Japanese.)
- Takahashi, M., Nakatani, S., Ito, Y., Takahashi, T., Zhang, X. W. & Ando, M. (1996). *Surf. Sci.* **357/358**, 78–81.
- Vlieg, E. (1997). *J. Appl. Cryst.* **30**, 532–543.